Fibers **2013**, *1*, 11-20; doi:10.3390/fib1020011

OPEN ACCESS

fibers

ISSN 2079-6439

www.mdpi.com/journal/fibers

Article

Er^{3+}/Ho^{3+}-Codoped Fluorotellurite Glasses for 2.7 μm Fiber Laser Materials

Yaoyao Ma [1,2], Feifei Huang [1,2,†], Lili Hu [1,†] and Junjie Zhang [1,*]

[1] Key Laboratory of Materials for High Power Laser, Shanghai Institute of Optics and Fine Mechanics, Chinese Academy of Sciences, Shanghai 201800, China; E-Mails: xiaoqi_198863@126.com (Y.M.); huangfeifei.88@163.com (F.H.); hulili@mail.siom.ac.cn (L.H.)

[2] Graduate School of Chinese Academy of Sciences, Beijing 100039, China

† These authors contributed equally to this work.

* Author to whom correspondence should be addressed; E-Mail: jjzhang@mail.siom.ac.cn; Tel.: +86-215-991-4297; Fax: +86-215-991-4516.

Received: 10 July 2013; in revised form: 6 August 2013 / Accepted: 12 August 2013 / Published: 16 August 2013

Abstract: This work reports the enhanced emission at 2.7 μm in Er^{3+}/Ho^{3+}-codoped fluorotellurite glass upon a conventional 980 nm laser diode. The significantly reduced green upconversion and 1.5 μm emission intensity in Er^{3+}/Ho^{3+}-codoped samples are observed. The results suggest that the Er^{3+}: $^4I_{13/2}$ state can be efficiently depopulated via energy transfer from Er^{3+} to Ho^{3+} and the detailed energy transfer mechanisms are discussed qualitatively. The energy transfer efficiency from Er^{3+}: $^4I_{13/2}$ to Ho^{3+}: $^5I_7$ is calculated to be as high as 67.33%. The calculated emission cross-section in Er^{3+}/Ho^{3+}-codoped fluorotellurite glass is 1.82×10^{-20} cm^2. This suggests that Er^{3+}/Ho^{3+}-codoped fluorotellurite glass is a potential material for 2.7 μm fiber laser.

Keywords: 2.7 μm; Er^{3+}/Ho^{3+}-codoped; fluorotellurite glass; energy transfer mechanism

1. Introduction

Owing to the increased interest in mid-infrared laser fiber (2–5 μm) used in laser surgery and remote chemical sensing fields, considerable researches have been performed to searching for new materials to use as hosts for mid-infrared laser hosts especially for Er^{3+} 2.7 μm [1,2]. Among many alternatives, fluoride fibers have emerged as natural candidates for mid-infrared laser materials because of their low phonon energy which decreases the rate of phonon-assisted nonradiative transitions [3,4]. However, fluoride fibers suffer from poor thermal stability and require complex fabrication route. Usually, the mid-infrared emission of Er^{3+} can hardly be observed in oxide glasses owing to the large phonon energy. However, it is well known that oxide glasses are more chemically and thermally stable. Among all the oxide glasses, tellurite glasses emerge as good candidates for mid-infrared fiber laser materials because of their lowest phonon energy (760 cm^{-1}) among all the oxide glasses with large refractive index and a broad transmission window (0.4–6 μm) [5–7].

Er^{3+} is an ideal luminescent center for 2.7 μm mid-infrared emission corresponding to the $^4I_{11/2} \rightarrow ^4I_{13/2}$ transition. However, Er^{3+} suffers from self-terminating of the $^4I_{11/2}$ level because of the much shorter lifetime of the emitting level ($^4I_{11/2}$) as compared to the terminal laser level ($^4I_{13/2}$). Fortunately, codoping with other ions such as Pr^{3+}, Nd^{3+}, Tm^{3+} and Ho^{3+} have been proved to be feasible alternatives to enhance the 2.7 μm emission [8–11]. The strong OH^- absorption around 3 μm is another important fact to obtain efficient Er^{3+} 2.7 μm emission. As is reported before [12], the addition of fluoride in the tellurite glasses was proved to be an effective way to reduce OH^{-1} groups and increase the radiative transition probabilities of 2.7 μm emission. Therefore, we prepare the Er^{3+}/Ho^{3+}-codoped fluorotellurite glass and evaluate the spectroscopic parameters based on the absorption spectra using the Judd-Ofelt theory. The detailed energy transfer processes based on the measured upconversion, near-infrared and mid-infrared fluorescence spectra are also discussed.

2. Experimental Section

The investigated fluorotellurite glasses in this study have the following molar compositions: $85TeO_2$-$10PbF_2$-$5LaF_3$-$1ErF_3$-$xHoF_3$(x = 0, 2), hereafter named TF glass. The samples were prepared using high-purity of powder. Well-mixed, 25 g batches of the samples were placed in an aluminum crucible and melted at 900 ℃ for 30 min. Then the melts were cast on a preheated steel plate and annealed for 3 h. at a temperature 10 ℃ below the Tg before they were naturally cooled to room temperature. The annealed samples were polished with a thickness of 1 mm for the optical property measurements.

The absorption spectra were recorded by a Perkin-Elmer Lambda 900 UV/VIS/NIR spectrophotometer in the wavelength range of 400–1700 nm. The fluorescence spectra were measured with an Edinburg FLSP920 type spectrometer upon excitation at 980 nm. The fluorescence lifetime was measured with the instrument FLSP920 (Edinburgh instruments Ltd., UK). All the measurements were carried out at room temperature.

3. Results and Discussion

3.1. Absorption Spectra and Judd-Ofelt Analyses

Figure 1 shows the absorption spectra of Er^{3+} singly and Er^{3+}/Ho^{3+}-codoped TF glasses. All the intrinsic absorption transitions of Er^{3+} and Ho^{3+} in the region from 300 to 1700 nm are retained and labeled in Figure 1. The strong absorption around 980 nm of the Er^{3+}/Ho^{3+}-codoped sample indicates that this glass can be excited efficiently by a 980 nm laser diode (LD). It can be seen that Er^{3+}: $^4F_{9/2}$, Ho^{3+}: $^5F_5$ and Er^{3+}: $^4S_{3/2}$, Ho^{3+}: ($^5S_2$ + $^5F_4$) are very close, which show that the energy transfer processes in Er^{3+}/Ho3+-codoped TF glasses are expected to be efficient.

Figure 1. Absorption spectra of Er^{3+} and Er^{3+}/Ho^{3+}-codoped samples.

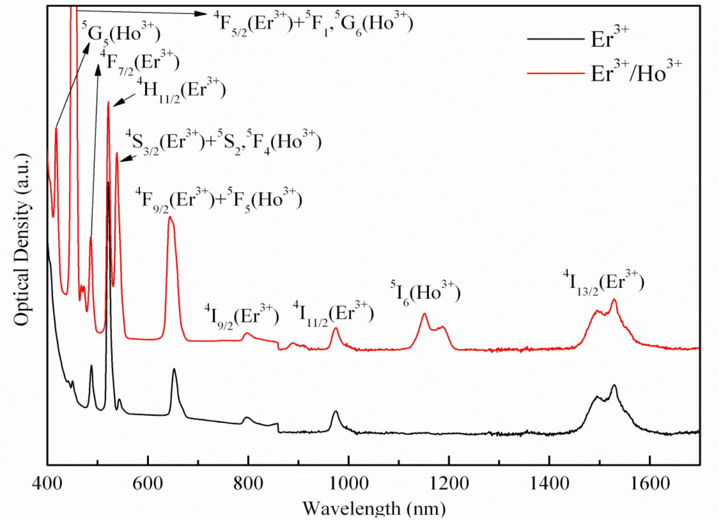

The Judd-Ofelt theory [13,14] has been commonly applied to determine the important spectroscopic and laser parameters of rare earth doped glasses. Judd-Ofelt theory has been described in other literature in detail [15]. Basically, the Judd-Ofelt analyses were applied using the experimental oscillator strengths of the absorption bands obtained from absorption spectra. Judd-Ofelt intensity parameters and oscillator strengths provide indirect information of the symmetry and bonding of rare-earth polyhedra within the matrix. Experimental (f_{mea}) and theoretical (f_{cal}) oscillator strength for representative transitions of Er in TF glass are tabulated in Table 1. Then the Judd-Ofelt intensity parameters, Ω_λ (λ = 2, 4, 6), can be derived using a least-square fitting approach and are shown in Table 2. Generally, Ω_λ is closely related to the structure change of the sites of rare earth ligand and the basicity of the glass network. It is hypersensitive to the change of composition of host materials. As is shown in Table 2, the calculated Ω_2 of Er^{3+} and Ho^{3+} in the present glass is lower than that other oxide glasses since the addition of fluoride in the tellurite glass can reduce the covalency and ligand of the glass matrix. The Ω_λ parameters follow the trend $\Omega_2 > \Omega_4 > \Omega_6$ in present TF glass. It should be mentioned that the root-mean-square is 2.98×10^{-6} for Er^{3+}/Ho^{3+}-codoped TF glass. The larger value of the fitting is due to the overlap of energy levels of Er^{3+} and Ho^{3+} we select to calculate the intensity parameters Ω_λ.

Table 1. Measured and calculated oscillator strength of Er^{3+} in TF glass.

Absorption	Wavelength (nm)	Oscillator strength (10^{-6})	
		Measured	**calculated**
$^4I_{15/2}\rightarrow{}^4I_{11/2}$	975	0.752	0.882
$^4I_{15/2}\rightarrow{}^4I_{9/2}$	799	0.344	0.496
$^4I_{15/2}\rightarrow{}^2H_{11/2}$	521	7.448	9.269
$^4I_{15/2}\rightarrow{}^4F_{7/2}$	488	3.784	3.139
$^4I_{15/2}\rightarrow{}^2G_{11/2}$	378	20.337	16.597

Table 2. Judd–Ofelt intensity parameters of Er^{3+} and Ho^{3+} in various glasses.

	$\Omega_t(10^{-20}\ cm^2)$	TF	Fluoride	Phosphate	Germanate	Silicate
Er^{3+}	Ω_2	3.83	2.98	6.65	5.81	4.23
	Ω_4	2.00	1.40	1.52	0.85	1.04
	Ω_6	1.37	1.04	1.11	0.28	0.61
	Ref.	This work	[16]	[17]	[17]	[17]
Ho^{3+}	Ω_2	3.80	1.86	5.60	6.66	5.84
	Ω_4	3.28	1.90	2.72	6.06	2.38
	Ω_6	1.10	1.32	1.87	2.26	1.75
	Ref.	This work	[18]	[19]	[20]	[21]

Table 3 represents the radiative transition probabilities (A_r), branching ratios (β) and radiative lifetime (τ_r) of certain levels of Er^{3+} ions which are calculated using the above obtained Judd-Ofelt intensity parameters. It is shown that the radiative probabilities A_r of Er^{3+}: $^4I_{11/2}\rightarrow{}^4I_{13/2}$ transition is 53.26 s^{-1} for Er^{3+}/Ho^{3+}-codoped samples.

Table 3. The radiative transition probability of electric dipolar transitions (A_{ed}), radiative transition probability of magnetic dipolar transitions (A_{md}), branching ratio (β) and radiative lifetime (τ_{rad}) of Er^{3+}/Ho^{3+}-codoped glasses.

Transitions	A_{ed} (s^{-1})	A_{md} (s^{-1})	Er^{3+}/Ho^{3+} β (%)	τ (ms)
$^4I_{13/2}\rightarrow{}^4I_{15/2}$	331.21	79.48	100.00	3.02
$^4I_{11/2}\rightarrow{}^4I_{15/2}$	317.20	0	83.47	2.63
$^4I_{13/2}$	62.80	22.51	16.53	
$^4I_{9/2}\rightarrow{}^4I_{15/2}$	319.89	0	74.63	2.33
$^4I_{13/2}$	104.17	0	24.30	
$^4I_{11/2}$	4.55	4.55	1.06	
$^4F_{9/2}\rightarrow{}^4I_{15/2}$	3,488.20	0	91.48	0.26
$^4I_{13/2}$	175.72	0	4.61	
$^4I_{11/2}$	144.22	0	3.78	
$^4I_{9/2}$	4.92	0	0.13	
$^4S_{3/2}\rightarrow{}^4I_{15/2}$	2,627.95	0	62.97	0.24
$^4I_{13/2}$	1,329.76	0	31.86	
$^4I_{11/2}$	82.77	0	1.98	
$^4I_{9/2}$	132.94	0	3.19	
$^2H_{11/2}\rightarrow{}^4I_{15/2}$	11,737.54	0	-	
$^4F_{7/2}\rightarrow{}^4I_{15/2}$	6,764.75	0	-	
$^4F_{5/2}\rightarrow{}^4I_{15/2}$	1,638.04	0	-	
$^2H_{9/2}\rightarrow{}^4I_{15/2}$	3,161.88	0	40.52	0.13
$^4I_{13/2}$	3,480.09	0	44.60	
$^4I_{11/2}$	1,042.72	0	13.36	
$^4I_{9/2}$	41.44	0	0.53	
$^4F_{9/2}$	77.59	0	0.99	

3.2. Fluorescence Spectra Analyses and Energy Transfer Mechanisms

Figure 2 presents the mid-infrared and near-infrared emission spectra of Er^{3+} and Er^{3+}/Ho^{3+}-codoped TF glasses under excitation at 980 nm. The emission at 2.7 μm corresponds to the transition of the Er^{3+}: $^4I_{11/2}\rightarrow{}^4I_{13/2}$. The emissions at 1.53 and 2.05 μm come from the transition of Er^{3+}: $^4I_{13/2}\rightarrow{}^4I_{15/2}$ and Ho^{3+}: $^5I_7\rightarrow{}^5I_8$, respectively. 2.7 μm emission can be observed in both kinds of samples. However, the intensity of the 2.7 μm increases with the addition of the HoF_3, which demonstrates the effective sensitization of Ho^{3+} ions.

Figure 2. Near-infrared and Mid-infrared fluorescence spectra of Er^{3+} and Er^{3+}/Ho^{3+}-codoped fluorotellurite glasses.

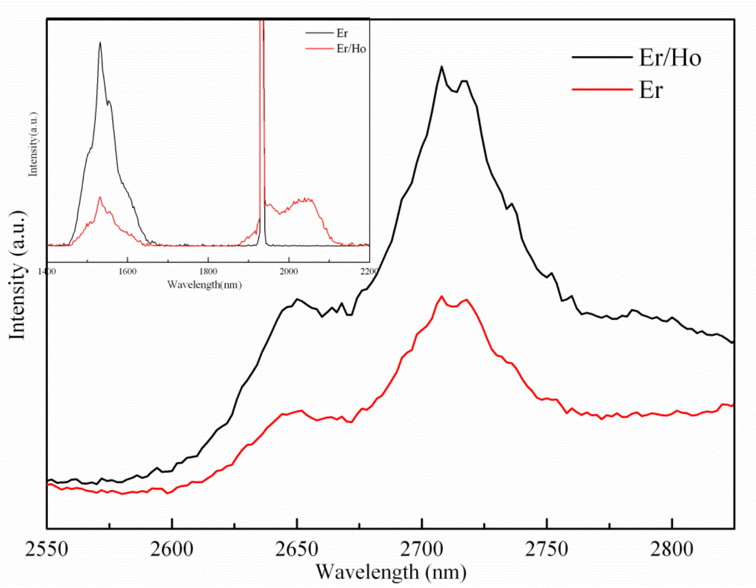

From the experimental phenomenon and theoretical data, possible mechanisms [22] for the emission bands are discussed based on the simplified energy levels of Er^{3+} and Ho^{3+} presented in Figure 3. Ions on the Er^{3+}: $^4I_{15/2}$ state are excited to the $^4I_{11/2}$ state by ground state absorption (GSA) when the sample is pumped by 980 nm LD. The involved energy transfer mechanisms processes based on the $^4I_{11/2}$ level are as follows: excited state absorption (ESA1), Er^{3+}: $^4I_{11/2}$ + a photon→Er^{3+}: $^4F_{7/2}$; ETU1, Er^{3+}: $^4I_{11/2}$ + $^4I_{11/2}\rightarrow{}^4I_{15/2}$ + $^4F_{7/2}$; ETU3, $^4I_{11/2}(Er^{3+})$ + $^5I_6(Ho^{3+})\rightarrow{}^4I_{15/2}(Er^{3+})$ + $^5F_4(Ho^{3+})$; $^4I_{11/2}\rightarrow{}^4I_{13/2}$ transition with 2.7 μm emission; ET1(a nonresonant process), from the Er^{3+}: $^4I_{11/2}$ level to the Ho^{3+}: $^5I_6$ level, energy excess (1470 cm^{-1}) is given to the matrix; non-radiatively relaxation to the Er^{3+}: $^4I_{13/2}$ level.

The Er^{3+}: $^4I_{13/2}$ level is populated owing to the nonradiative relaxation from the upper $^4I_{11/2}$ level. There exist four main energy transfer processes for the Er^{3+}: $^4I_{13/2}$ level in present glass as follows: excited state absorption (ESA2), Er^{3+}: $^4I_{13/2}$ + a photon→Er^{3+}: $^4I_{9/2}$; ETU2 [23], Er^{3+}: $^4I_{13/2}$ + $^4I_{13/2}\rightarrow{}^4I_{15/2}$ + $^4F_{9/2}$; ETU4, $^4I_{13/2}$ (Er^{3+}) + $^5I_6(Ho^{3+})\rightarrow{}^4I_{15/2}(Er^{3+})$ + $^5F_5(Ho^{3+})$; $^4I_{13/2}\rightarrow{}^4I_{15/2}$ transition with 1.5 μm emission; ET2(a nonresonant process), from the Er^{3+}: $^4I_{13/2}$ level to the Ho^{3+}: $^5I_7$ level, energy excess (1398 cm^{-1}) is given to the matrix. After ET2 process, 2.05 μm emission can be observed due to the Ho^{3+}: $^5I_7\rightarrow{}^5I_8$. The ESA2 process populates the Er^{3+}: $^4F_{9/2}$ level which relaxes radiatively to the ground state with red emission around 660 nm and non-radiatively to the next lower

Er^{3+}: $^4I_{9/2}$ level. The energy stored in the Er^{3+}: $^4I_{9/2}$ can partly be non-radiatively decayed to the Er^{3+}: $^4I_{11/2}$ level, which is beneficial to the 2.7 μm emission.

Figure 3. Energy level schemes of Er^{3+} and Ho^{3+} and energy transfer sketch map between Er^{3+} and Ho^{3+}.

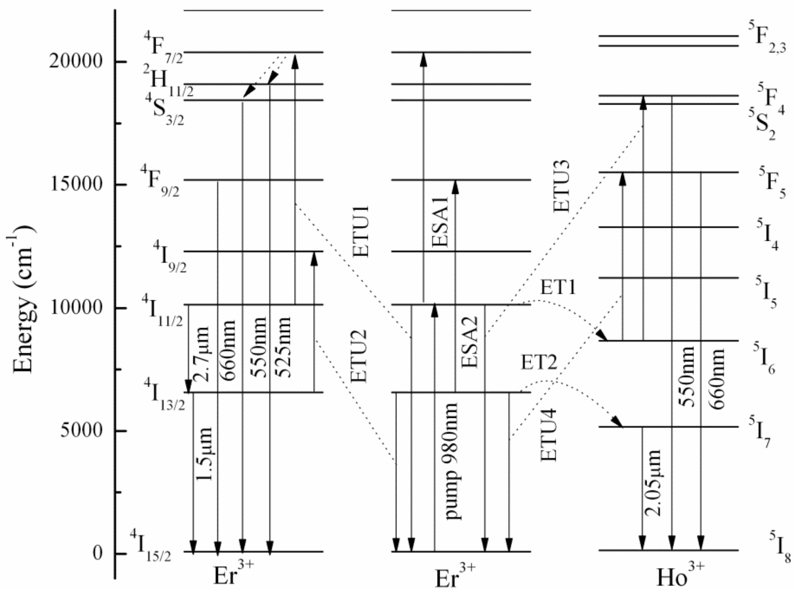

The visible emission spectra for Er^{3+} doped and Er^{3+}/Ho^{3+}-codoped glasses upon 980 nm excitation are shown in Figure 4. Three visible emission peaks centered at 525, 550 and 660 nm are observed. As discussed above, the stored energy in the $^4F_{7/2}$ level after ESA1 process decays non-radiatively to the lower levels $^2H_{11/2}$ and $^4S_{3/2}$. Then the Er^{3+}: $(^2H_{11/2} + {}^4S_{3/2}) \rightarrow {}^4I_{15/2}$ transitions bring green emissions (525 and 548 nm). Meanwhile, the excited Ho^{3+} ions at ($^5S_2$ + $^5F_4$) and $^5F_5$ levels also generate 550 and 660 nm emissions, respectively. It is noted that the fluorescence intensity of red emissions becomes stronger when codoped with Ho^{3+} while the green emission becomes weaker. Because the energy gaps of the ET1 and ET2 process are relatively small, so both processes can happen efficiently. It is expected that the ESA1 and ESA2 processes will be reduced while the sample is codoped with Ho^{3+}, so part of green and red emission can be attributed to the Ho^{3+} upconversion emissions. Since the energy gap of the ET2 process is smaller than that of ET1 process, the energy transfer efficiency of ET2 is expected to be higher than that of ET1, this is also proved from the extremely decreased 1.5 μm emission in the Er^{3+}/Ho^{3+}-codoped samples, consequently ions on the $^5I_7$ level are much more than that on the $^5I_6$ level. Then the $^5F_5$ level that is populated through ETU4 generates stronger 660 nm emission while the $^5S_2$ ($^5F_4$) levels that are populated through ETU3 generate weaker 550 nm emission.

3.3. Fluorescence Spectra Analyses and Energy Transfer Mechanisms

The energy transfer efficiency has been estimated from the measured lifetime of the 1.53 μm emission of Er^{3+} singly and Er^{3+}/Ho^{3+}-codoped samples by the following formula [24]:

$$\eta_t = 1 - \frac{\tau_{EH}}{\tau_E} \quad (1)$$

where τ_{EH} and τ_E are the Er^{3+} lifetime monitored at 1.53 μm with and without Ho^{3+} ions, respectively. The lifetime decay curves of the Er^{3+}: $^4I_{13/2}$ level with and without Ho^{3+} in TF glasses are measured and shown in Figure 5. The values for lifetime of Er^{3+}: $^4I_{13/2}$ level for Er^{3+} and Er^{3+}/Ho^{3+}-codoped samples are 5.25 ms and 1.71 ms, respectively. The decrease of lifetime of the Er^{3+}: $^4I_{13/2}$ state indicates the existence of ET2 process. In addition, the energy transfer efficiency from the Er^{3+}: $^4I_{13/2}$ to Ho^{3+}: $^5I_7$ level is calculated to be 67.33%.

Figure 4. Upconversion emission spectra of Er^{3+} and Er^{3+}/Ho^{3+}-codoped glass samples.

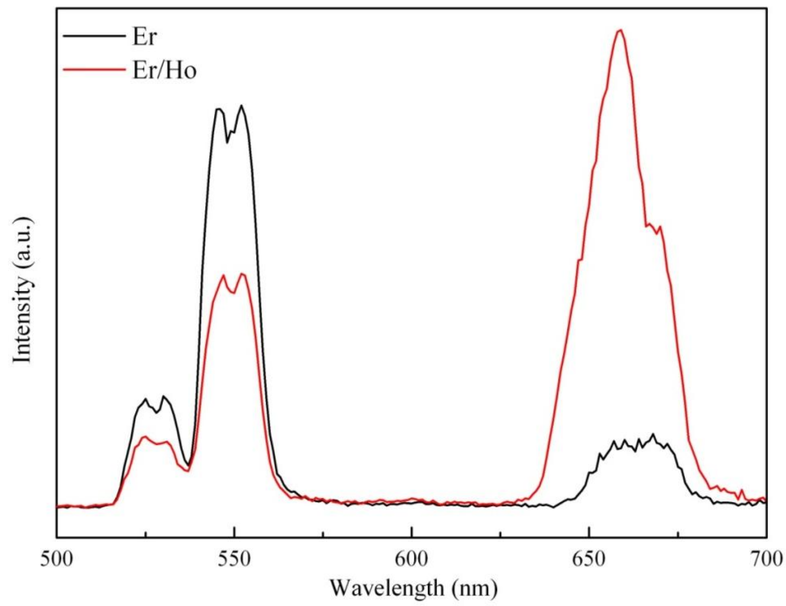

Figure 5. Fluorescence decay curves of Er^{3+}: $^4I_{13/2}$ level in Er^{3+} singly and Er^{3+}/Ho^{3+}-codoped samples.

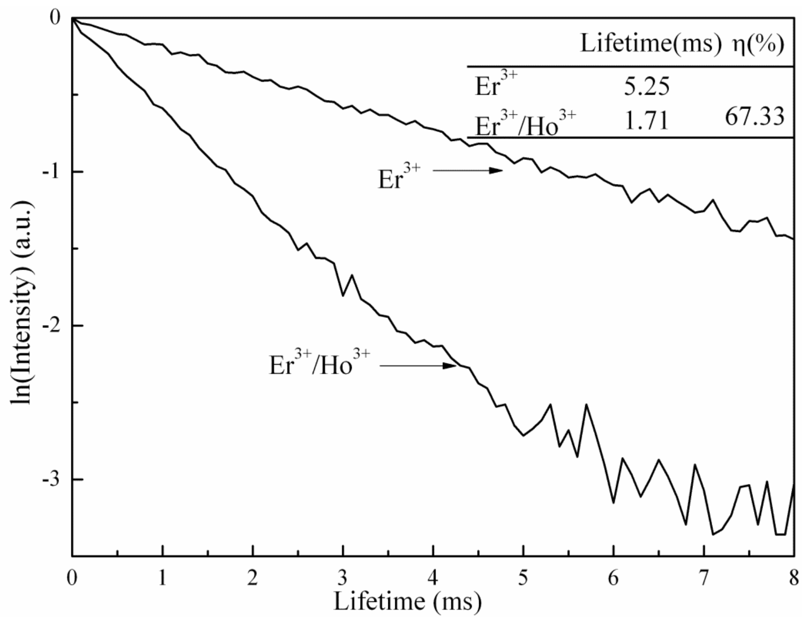

3.4. Cross-Sections Analyses

The emission cross section is an important factor for evaluating the emissive ability of luminescent center. The absorption and emission cross sections could be calculated from Füchtbauer–Ladenburg equation [25] and McCumber theory [26]:

$$\sigma_{em}(\lambda) = \frac{\lambda^4 A_{rad}}{8\pi c n^2} \times \frac{\lambda I(\lambda)}{\int \lambda I(\lambda) d\lambda} \tag{2}$$

$$\sigma_{em}(\lambda) = \sigma_{abs}(\lambda)(Z_L/Z_U)\exp[(\varepsilon - h\nu)/kT] \tag{3}$$

where λ is the wavelength, A_{rad} is the spontaneous transition probability, I(λ) is the fluorescence spectra intensity, n and c represent the refractive index and the speed of light, Z_L and Z_U are partition functions of the lower and upper manifolds, respectively. The maximum absorption (σ_{abs}) and emission cross section (σ_{em}) (both peaking at 2708 nm) in Figure 6 are 1.54×10^{-20} cm^2 and 1.82×10^{-20} cm^2, respectively, which is larger than the values reported in Ref. [27–29]. Hence, Er^{3+}/Ho^{3+}-codoped TF glass with promising properties has potential applications for 2.7 μm laser material.

Figure 6. Absorption and emission cross sections of Er^{3+}: $^4I_{11/2} \rightarrow {}^4I_{13/2}$ in TF glasses.

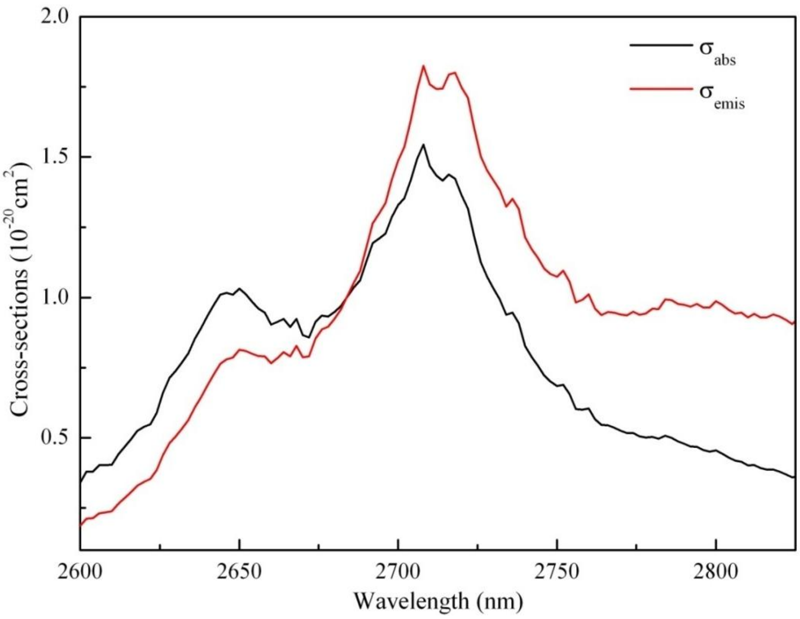

4. Conclusions

Enhanced 2.7 μm emission was obtained in Er^{3+}/Ho^{3+}-codoped fluorotellurite glass. This suggests that Ho^{3+} can be a feasible approach to obtain efficient Er^{3+} 2.7 μm emission pumped by common 980 nm LD in fluorotellurite glass for practical applications. It was also found that the green upconversion and 1.5 μm emissions extremely decreased in the Er^{3+}/Ho^{3+}-codoped glass. The energy transfer mechanisms between Er^{3+} and Ho^{3+} were discussed in detail and the energy transfer efficiency was calculated to be 67.33%. Larger absorption and emission cross sections of Er^{3+}: $^4I_{11/2} \rightarrow {}^4I_{13/2}$ in TF glasses were obtained which were 1.54×10^{-20} cm^2 and 1.82×10^{-20} cm^2, respectively. These results suggest that Er^{3+}/Ho^{3+}-codoped fluorotellurite glass has potential applications for 2.7 μm fiber laser materials.

Acknowledgments

This research was financially supported by the Chinese National Natural Science Foundation (No. 51172252).

Conflicts of Interest

The authors declare no conflicts of interest.

References

1. Zhu, X.; Jain, R. 10W level diode-pumped compact 2.78 μm ZBLAN fiber laser. *Opt. Lett.* **2007**, *32*, 26–28.
2. Sanghera, J.S.; Shaw, L.B.; Aggarwal, I.D. Chalcogenide Glass-Fiber-Based Mid-IR Sources and Applications. *IEEE J. Sel. Top. Quant.* **2009**, *15*, 114–119.
3. Jackson, S.D.; King, T.A.; Pollnau, A.M. Diode-pumped 1.7 W erbium 3 μm fiber laser. *Opt. Lett.* **1999**, *24*, 1133–1135.
4. Tokita, S.; Murakami, M.; Shimizu, S.; Hashida, M.; Sakabe, S. Liquid-cooled 24 W mid-infrared Er^{3+}:ZBLAN fiber laser. *Opt. Lett.* **2009**, *34*, 3062–3064.
5. Wang, J.S.; Vogel, E.M.; Snitzer, E. Tellurite glass: a new candidate for fiber devices. *Opt. Mater.* **1994**, *3*, 187–203.
6. Richards, B.; Tsang, Y.; Binks, D.; Lousteau, J.; Jha, A. Efficient ~2um Tm^{3+}-doped tellurite fiber laser. *Opt. Lett.* **2008**, *33*, 402–404.
7. Mori, A.; Ohishi, Y.; Sudo, S. Erbium-doped tellurite glass fibre laser and amplifier. *Electron. Lett.* **1997**, *33*, 863–864.
8. Golding, P.S.; Jackson, S.D.; King, T.A.; Pollnau, M. Energy transfer processes in Er^{3+}-doped and Er^{3+},Pr^{3+}-codoped ZBLAN glasses. *Phys. Rev. B* **2000**, *62*, 856–864.
9. Chou, Y.G.; Kim, K.H.; Lee, B.J.; Shin, Y.B.; Kim, Y.S.; Heo, J. Emission properties of the Er^{3+}:$^4I_{11/2–4}I_{13/2}$ transition in Er^{3+} and Er^{3+}/Tm^{3+}-codoped Ge-Ga-As-S glasses. *J. Non-Cryst. Solids* **2000**, *278*, 137–144.
10. Zhong, H.; Chen, B.; Ren, G.; Cheng, L.; Yao, L.; Sun, J. 2.7 μm emission of Nd^{3+}, Er^{3+}codoped tellurite glass. *J. Appl. Phys.* **2009**, *106*, 083114.
11. Zhang, L.; Yang, Z.; Tian, Y.; Zhang, J.; Hu, L. Comparative investigation on the 2.7 μm emission in Er^{3+}/Ho^{3+} codoped fluorophosphate glass. *J. Appl. Phys.* **2011**, *110*, 093106.
12. O'Donnell, M.D.; Miller, C.A.; Furniss, D.; Tikhomirov, V.K.; Seddon, A.B. Fluorotellurite glasses with improved mid-infrared transmission. *J. Non-Cryst. Solids* **2003**, *331*, 48–57.
13. Ofelt, S.G. Intensities of Crystal Spectra of Rare-Earth Ions. *J. Chem. Phys.* **1962**, *37*, 511.
14. Judd, B.R. Optical Absorption Intensities of Rare-Earth Ions. *Phys.l Rev.* **1962**, *127*, 750–761.
15. Xu, R.R.; Tian, Y.; Wang, M.; Hu, L.L.; Zhang, J.J. Spectroscopic properties of 1.8 μm emission of thulium ions in germanate glass. *Appl. Phys. B* **2010**, *102*, 109–116.

16. Ivanova, S.; Pelle, F. Strong 1.53 μm to NIR-VIS-UV upconversion in Er-doped fluoride glass for high-efficiency solar cells. *J. Opt. Soc. Am. B* **2009**, *26*, 1930–1938.
17. Zou, X.; Izumitani, T. Spectroscopic properties and mechanisms of excited state absorption and energy transfer upconversion for Er^{3+}-doped glasses. *J. Non-Cryst. Solids* **1993**, *162*, 68–80.
18. Peng, B.; Izumitani, T. Optical properties, fluorescence mechanisms and energy transfer in Tm^{3+}, Ho^{3+} and Tm^{3+}-Ho^{3+} doped near-infrared laser glasses, sensitized by Yb^{3+}. *Opt. Mater.* **1995**, *4*, 797–810.
19. Reisfeld, R.; Hormadaly, J. Optical intensities of holmium in tellurite, calibo, and phosphate glasses. *J. Chem. Phys.* **1976**, *64*, 3207–3212.
20. Xu, R.; Pan, J.; Hu, L.; Zhang, J. 2.0 μm emission properties and energy transfer processes of Yb^{3+}/Ho^{3+} codoped germanate glass. *J. Appl. Phys.* **2010**, *108*, 043522.
21. Feng, L.; Wang, J.; Tang, Q.; Liang, L.; Liang, H.; Su, Q. Optical properties of Ho^{3+}-doped novel oxyfluoride glasses. *J. Lumin.* **2007**, *124*, 187–194.
22 Zhang, X.D.; Xu, T.F.; Dai, S.X.; Nie, Q.H.; Shen, X.; Lu, L.; Zhang, X.H. Investigation of energy transfer and frequency upconversionin Er^{3+}/Ho^{3+} co-doped tellurite glasses. *J. Alloy Compd.* **2008**, *450*, 306–309.
23. Pollnan, M. The route toward a diode-pumped 1 W erbium 3 μm fiber laser. *IEEE J. Sel. Top. Quant.* **1997**, *33*, 1982–1990.
24. Carnall, W.T.; Fields, P.R.; Rajnak, K. Spectral Intensities of the Trivalent Lanthanides and Actinides in Solution. II. Pm^{3+}, Sm^{3+}, Eu^{3+}, Gd^{3+}, Tb^{3+}, Dy^{3+}, and Ho^{3+}. *J. Chem. Phys.* **1968**, *49*, 4412–4423.
25. Stephen, A.P.; Chase, L.L.; Smith, L.K.; Kway, W.L.; Krupke, W.F. Infrared Cross—Section Measurements for Crystals Doped with Er^{3+}, Tm^{3+}, and Ho^{3+}. *IEEE J. Quantum Elect.* **1992**, *28*. 2619–2630.
26. McCumber, D.E. Theory of Phonon Terminated Optical Masers. *Phy. Rev.* **1964**, *134*, A299–A306.
27. Guo, Y.; Tian, Y.; Zhang, L.; Hu, L.; Chen, N.K.; Zhang, J. Pr^{3+}-sensitized Er^{3+}-doped bismuthate glass for generating high inversion rates at 2.7 μm wavelength. *Opt. Lett.* **2012**, *37*, 3387–3389.
28. Tian, Y.; Xu, R.; Zhang, L.; Hu, L.; Zhang, J. Observation of 2.7 μm emission from diode-pumped Er^{3+}/Pr^{3+}-codoped fluorophosphate glass. *Opt. Lett.* **2011** *36*, 109–111.
29. Tikhomirov, V.K.; Méndez-Ramos, J.; Rodríguez, V.D.; Furniss, D.; Seddon, A.B. Laser and gain parameters at 2.7 μm of Er^{3+}-doped oxyfluoride transparent glass–ceramics. *Opt. Mater.* **2006**, *28*, 1143–1146.